Supporting Information for

Causal influences of El Niño–Southern Oscillation on global dust activities

Thanh Le[1⋆] and Deg-Hyo Bae[1⋆]

[1]Department of Civil and Environmental Engineering, Sejong University, Seoul 05006, Republic of Korea

⋆Corresponding author(s): Deg-Hyo Bae (dhbae@sejong.ac.kr) and Thanh Le (levinhthanh.lvt@gmail.com)

Contents of this Supporting Information

Text S1

We use the following multivariate predictive model (Mosedale et al., 2006; Stern and Kaufmann, 2013) to estimate the causal links between the ENSO and dust deposition:

$$\boldsymbol{X_t} = \sum_{i=1}^{p} \boldsymbol{\alpha_i X_{t-i}} + \sum_{i=1}^{p} \boldsymbol{\beta_i Y_{t-i}} + \sum_{j=1}^{m} \sum_{i=1}^{p} \boldsymbol{\delta_{j,i} Z_{j,t-i}} + \boldsymbol{\varepsilon_t} \quad \textbf{(1)}$$

where X_t is the annual mean (or seasonal mean) dust deposition for year t, Y_t is the ENSO index, and $Z_{j,t}$ is the confounding factor j for year t. In the predictive model shown in equation 1, while estimating the influence of Y on X (i.e., the contribution of the term $\sum_{i=1}^{p} \beta_i Y_{t-i}$ in predicting X), the contribution of past X events are already taken into account by adding the term $\sum_{i=1}^{p} \alpha_i X_{t-i}$. Thus, the causal influence of Y on X, if detected, is robust and the contribution of past X events are already considered in our analyses. Here, m is number of confounding factors and $p \geq 1$ is the order of the multivariate predictive model. The optimal order p is less than 8 (p is an integer with units of year, computed by minimizing the Schwarz criterion or the Bayesian information criterion (Schwarz, 1978)), hence, the connection between dust deposition and ENSO is investigated at interannual timescales. The optimal orders might be different for each model.

The ENSO index was computed as the average sea surface temperature (SST) anomalies in the Niño 3.4 area (120–170°W; 5°N–5°S) in boreal winter (December–January–February, DJF). Confounding factors (i.e., the dipole mode index (DMI; Saji et al., 1999), the Southern Annular Mode (SAM) and the North Atlantic Oscillation (NAO; e.g., Hurrell et al., 2003)) may have effects on the connections between ENSO and dust deposition. The DMI was given as the difference in boreal fall (September–October–November, SON) SST anomalies between two Indian Ocean regions of the western pole (50–70°E; 10°N–10°S) and southeastern pole (90–110°E; 0°N–10°S). The SAM (Cai et al., 2011) was calculated as the first empirical orthogonal function (EOF) of the boreal summer (June–July–August, JJA) sea level pressure (SLP) anomalies for the region of 40–70°S. The NAO index is computed as the EOF of boreal winter (DJF) SLP anomalies in the North Atlantic area (90ºW-40ºE, 20º-70ºN).

Here we consider the simultaneous impacts of confounding factors and thus provide more information of the real-world teleconnections. Our analysis uses three different confounding factors; thus, m is equal to 3. The noise residuals ε_t and the regression coefficients α_i, β_i and $\delta_{j,i}$

are the results of the multiple linear regression analysis using the least squares method. We detrend and normalize all the climate indices.

We estimate the probability of no Granger causality by applying a test of Granger causality (Le and Bae, 2020; Mosedale et al., 2006; Stern and Kaufmann, 2013) for the multivariate predictive model shown in equation 1.

For computing the degree of uncertainty, we followed recent guidance (Stocker et al., 2013) and utilized the terms 'very unlikely', 'unlikely', 'likely' for the 0–10%, 0–33%, and 66–100% probability of the likelihood of the outcome, respectively. For example, if the *p*-value is less than 0.33, the result indicates that ENSO is unlikely to display no Granger causality on dust deposition. In this instance, we conclude that ENSO has 'causal effect' on dust deposition.

References

Cai, W., Sullivan, A. and Cowan, T.: Interactions of ENSO, the IOD, and the SAM in CMIP3 Models, J. Clim., 24(6), 1688–1704, doi:10.1175/2010JCLI3744.1, 2011.

Hurrell, J. W., Kushnir, Y., Ottersen, G. and Visbeck, M.: An overview of the North Atlantic Oscillation, in Geophysical Monograph American Geophysical Union, pp. 1–35, American Geophysical Union., 2003.

Le, T. and Bae, D.-H.: Response of global evaporation to major climate modes in historical and future Coupled Model Intercomparison Project Phase 5 simulations, Hydrol. Earth Syst. Sci., 24(3), 1131–1143, doi:10.5194/hess-24-1131-2020, 2020.

Mosedale, T. J., Stephenson, D. B., Collins, M. and Mills, T. C.: Granger Causality of Coupled Climate Processes: Ocean Feedback on the North Atlantic Oscillation, J. Clim., 19(7), 1182–1194, doi:10.1175/JCLI3653.1, 2006.

Saji, N. H., Goswami, B. N., Vinayachandran, P. N. and Yamagata, T.: A dipole mode in the tropical Indian Ocean, Nature, 401(6751), 360–363, doi:10.1038/43854, 1999.

Schwarz, G.: Estimating the dimension of a model, Ann. Stat. [online] Available from: http://projecteuclid.org/euclid.aos/1176344136 (Accessed 30 May 2014), 1978.

Stern, D. I. and Kaufmann, R. K.: Anthropogenic and natural causes of climate change, Clim. Change, 122(1–2), 257–269, doi:10.1007/s10584-013-1007-x, 2013.

Stocker, T. F., Qin, D., Plattner, G.-K., Alexander, L. V., Allen, S. K., Bindoff, N. L., Bréon, F.-M., Church, J. A., Cubasch, U., Emori, S., Forster, P., Friedlingstein, P., Gillett, N., Gregory, J. M., Hartmann, D. L., Jansen, E., Kirtman, B., Knutti, R., Kumar, K. K., Lemke, P., Marotzke, J., Masson-Delmotte, V. Meehl, G. A., Mokhov, I. I., Piao, S., Ramaswamy, V., Randall, D., Rhein, M., Rojas, M., Sabine, C., Shindell, D., Talley, L. D., Vaughan, D. G. and Xie, S.-P.: Technical Summary, in Climate Change 2013 - The Physical Science Basis, edited by Intergovernmental Panel on Climate Change, pp. 31–116, Cambridge University Press, Cambridge., 2013.

77

Table S1. List of CMIP6 models used in this study.

No.	Model name	Modelling center, country	Aerosol model	Atmospheric Chemistry model
1	CanESM5	CCCma, Canada	Interactive	Specified oxidants for aerosols
2	CESM2	NCAR, United States	MAM4	MAM4
3	CESM2_FV2	NCAR, United States	MAM4	MAM4
4	CESM2_WACCM	NCAR, United States	MAM4	MAM4
5	CESM2_WACCM_FV2	NCAR, United States	MAM4	MAM4
6	CNRM_ESM2_1	CNRM-CERFACS, France	TACTIC_v2	REPROBUS-C_v2
7	GFDL_ESM4	NOAA-GFDL, United States	Interactive	GFDL-ATMCHEM4.1
8	INM-CM4-8	INM, Russia	INM-AER1	None
9	INM-CM5-0	INM, Russia	INM-AER1	None
10	MIROC-ES2L	MIROC Japan	SPRINTARS6.0	None
11	MIROC6	MIROC, Japan	SPRINTARS6.0	None
12	UKESM1_0_LL	MOHC NERC, United Kingdom	UKCA-GLOMAP-mode	UKCA-StratTrop

Table S2. List of CMIP6 models used in this study with available data denoted by a check mark (✓). The data unavailable are denoted by a cross (×).

No.	Model name	Modelling center, country	dry dust	wet dust	od550dust	emidust
1	CanESM5	CCCma, Canada	✓	✓	✓	✓
2	CESM2	NCAR, United States	✓	✓	✓	✓
3	CESM2_FV2	NCAR, United States	✓	✓	✓	✓
4	CESM2_WACCM	NCAR, United States	✓	✓	✓	✓
5	CESM2_WACCM_FV2	NCAR, United States	✓	✓	✓	✓
6	CNRM_ESM2_1	CNRM-CERFACS, France	✓	✓	×	✓
7	GFDL_ESM4	NOAA-GFDL, United States	✓	✓	×	×
8	INM-CM4-8	INM, Russia	✓	✓	✓	✓
9	INM-CM5-0	INM, Russia	✓	✓	✓	✓
10	MIROC-ES2L	MIROC Japan	✓	✓	×	✓
11	MIROC6	MIROC, Japan	✓	✓	✓	✓
12	UKESM1_0_LL	MOHC NERC, United Kingdom	✓	✓	✓	✓

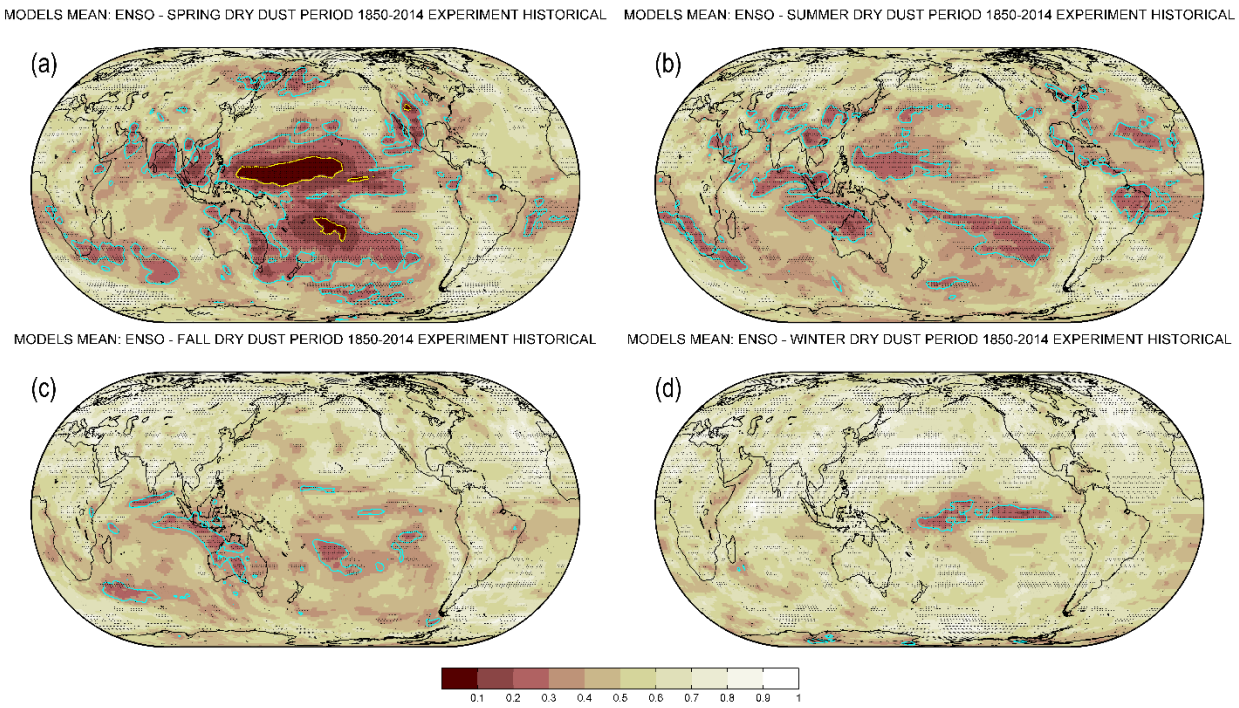

Figure S1. Multi-model mean probability map of no Granger causality from ENSO [DJF] to the following seasonal mean dry dust deposition over the period 1850-2014 of the historical simulation. (a) Spring [MAM]. (b) Summer [JJA]. (c) Fall [SON]. (d) Winter [DJF]. Stippling demonstrates that at least 70% of total models show agreement on the mean probability of all models at a given grid point. The cyan and yellow contour lines signify *p*-value = 0.33 and 0.1, respectively. Brown shades denote a low probability for the absence of Granger causality. ENSO: El Niño–Southern Oscillation.

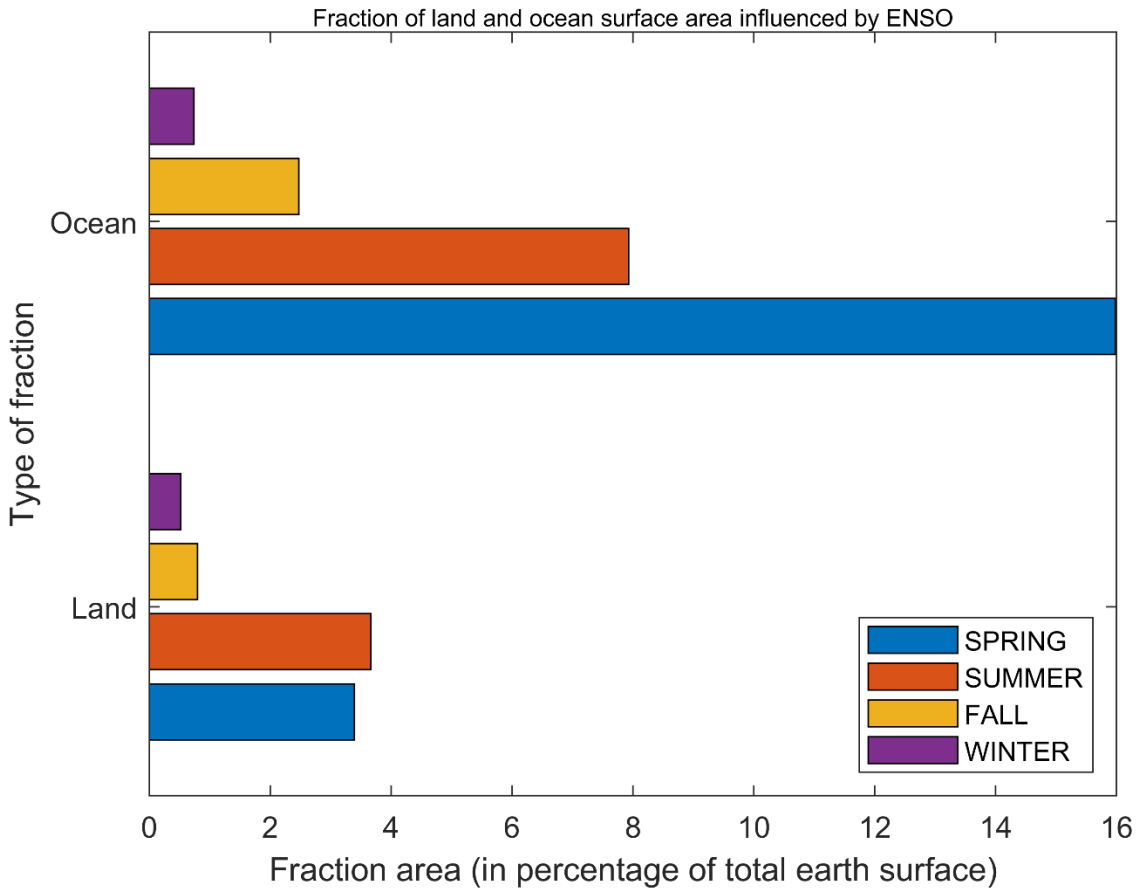

Figure S2. Fraction of total Earth-surface over land and ocean with probability for no Granger causality from ENSO to seasonal mean dry dust deposition lower than 0.33 (i.e., *p*-value < 0.33). Fraction areas influenced by ENSO on Spring, Summer, Fall and Winter dry dust deposition are displayed in blue, red, yellow, and purple bars, respectively. ENSO: El Niño–Southern Oscillation.

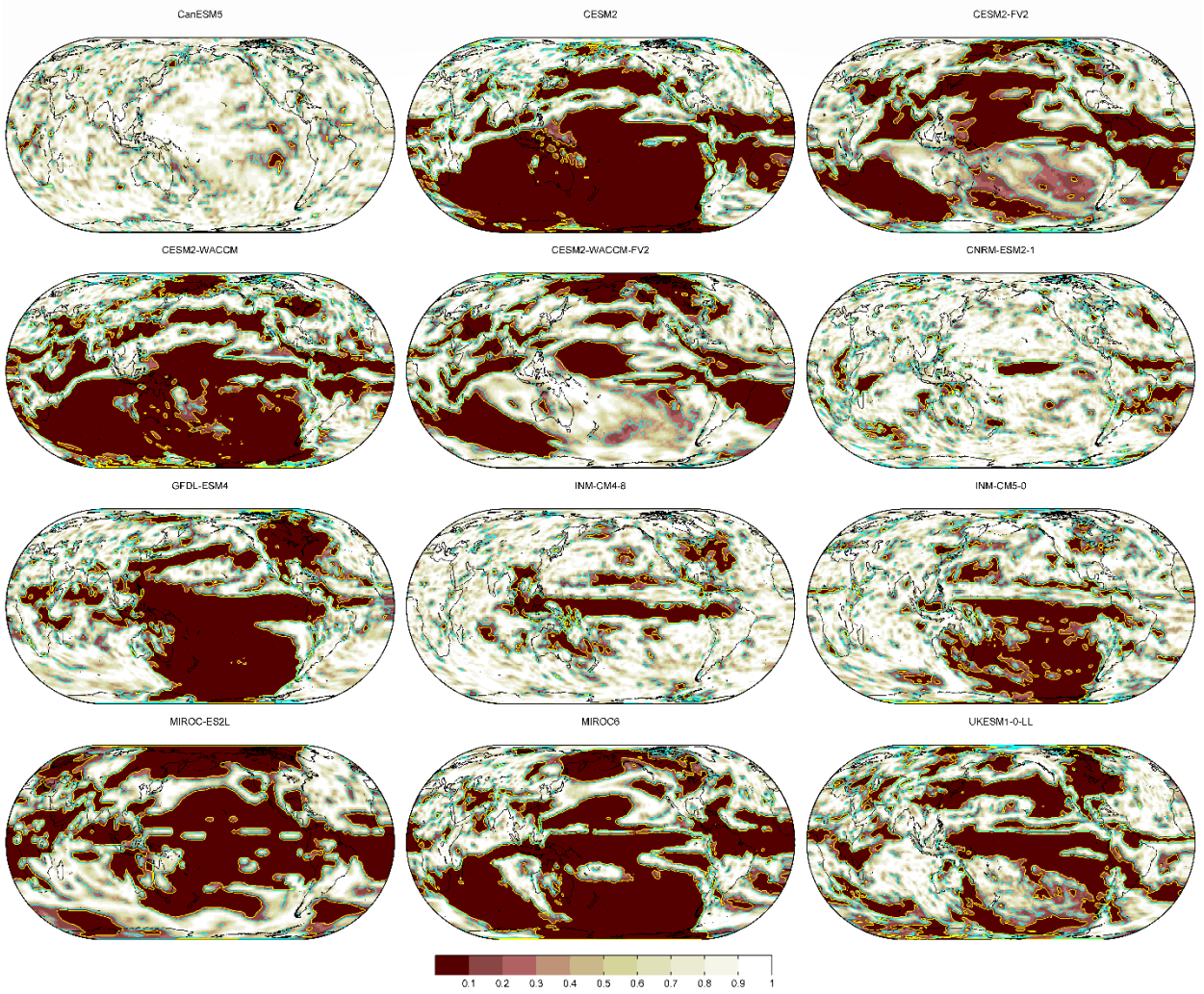

Figure S3. As in Figure 1, but for the probability of no Granger causality of ENSO on annual mean wet dust deposition over the period 1850-2014 for the historical simulation of 12 individual models (see Tables S1 and S2). ENSO: El Niño–Southern Oscillation.